Progress In Electromagnetics Research B, Vol. 64, 47–62, 2015

Design of a Compact Orthogonal Broadband Printed MIMO Antennas for 5-GHz ISM Band Operation

Dhirgham K. Naji*

Abstract—This paper presents a new design approach for compact orthogonal broadband printed multiple-input multiple-output (MIMO) antennas based on a coplanar waveguide (CPW)-fed hexagonal-ring monopole antenna (HRMA) element. The design procedure of the basic radiating element is initiated from a stripline (SL)-fed circular monopole antenna (CMA). Then various antennas involved in the design evolution process are introduced to attain a compact CPW-fed HRMA. This basic antenna element has a compact size of $13 \times 10\,\text{mm}^2$, 50% smaller than SL-fed CMA, and a prototype of this antenna is built and tested. Based on HRMA element, compact two- and four-element MIMO antenna systems are designed, fabricated and experimentally demonstrated for 5-GHz ISM band operation. The MIMO antenna systems use orthogonally configured of identical closely spaced HRMA elements, with CPW-fed printed on one side of the substrate to achieve good isolation. Design simulation is carried out with the aid of Computer Simulation Technology Microwave Studio (CST MWS) and confirmed with High Frequency Structure Simulator (HFSS). The experimental results are in close agreement with the simulated ones, which validates the design principle. Based on experimental results, the two MIMO antenna systems have an impedance bandwidth of more than 2 GHz, good isolation of less than 15 dB, and a low envelope correlation coefficient of better than −26 dB across the frequency band of (4–6 GHz), which are suitable for 5-GHz MIMO applications.

1. INTRODUCTION

With the increasing demand of high data transmission rates, overcoming the limited channel capacity and improving the reliability and data throughput, multiple-input multiple-output (MIMO) systems are being widely used in the communication systems and have attracted great interest of researchers [1]. It is well known that a MIMO system utilizing more than one antenna element is more preferable than single-input single-output (SISO) in an aspect of increasing channel capacity and without using extra spectrum and transmit power [2]. Because of these aforementioned features, the MIMO technology has been remarkably widespread to latest mobile communication standards such as long-term evolution (LTE), worldwide interoperability for microwave access (WiMAX) and wireless local area network (WLAN). Therefore, it is necessary to incorporate compact-size and high-performance antennas with wide-impedance bandwidth to wireless personal communication terminals [3]. However, designing compact radiating antenna elements within the restricted size of the system while maintaining a good isolation between multiple antennas are usually a challenging task. Since mutual coupling between closely spaced antenna elements of the MIMO system results in the decrease of radiation efficiency due to impedance mismatch, which deteriorates MIMO system performances [4]. Moreover, mutual coupling may increase correlation between channels and lead to reduced system capacity. As a result, MIMO

Received 21 September 2015, Accepted 1 November 2015, Scheduled 6 November 2015
* Corresponding author: Dhirgham Kamal Naji (dknaji73@yahoo.com).
The author is with the Department of Electronic and Communications Engineering, College of Engineering, Al-Nahrain University, Baghdad, Iraq.

antennas have to satisfy all the performance indicators of a single-element antenna while providing good mutual coupling between closely placed antenna elements [5].

During the recent years, numerous designs of MIMO antenna systems have been investigated for wireless applications and are mainly focused on sufficiently minimizing the effect of mutual coupling between radiating elements and presenting different convenient techniques in order to implement an efficient and compact MIMO system [6–14]. These systems were developed for various bands including single and/or dual band, GSM band, LTE band, WiMAX band, and two ISM bands covering 2.45 GHz and/or 5 GHz band. The proposed methods for reducing mutual coupling included employing a simple microstrip patch element in between the antennas [6], using parasitic coupling elements between the radiators [7, 8], connecting the elements employing a neutralization line [9, 10], introducing resonators between the antenna elements [11], placing the antenna elements in an orthogonal configuration [12, 13] and metamaterial-based antennas [14]. Alternatively, Electromagnetic Band Gap (EBG) cells [15] and partially extended ground [PEG] plane [16] may be used to eliminate coupling. However, designing the radiating elements as well as parasitic structures, neutralization line, EBG cells, PEG plane, and metamaterial structures requires considerable additional efforts. This paper uses orthogonal configuration technique in designing MIMO antenna system to achieve reduced mutual coupling between antenna elements reducing the efforts and complexities resulting from employing the aforementioned methods.

A lot of wireless communication devices such as mobile phones, laptops, and tablets use the WLAN to access many internet services. Two bands were adopted as a new standard by IEEE 802.11ac for WLAN operations, which deal with the data rates up to a minimum of approximately 1 Gb/s and a maximum around 7 Gb/s (may be considered as 5G Wi-Fi), the traditional 2.45 GHz band and the new 5 GHz band [17]. On the other hand, using antenna miniaturization techniques for designing compact antennas yields low antenna bandwidth, efficiency, and gain. Also, as stated before, in the design of a compact MIMO antenna system, it is necessary to use antenna miniaturization techniques that keep the antenna design simple while maintaining the diversity performance as high as possible although the antenna elements are placed close to each other. So far, many miniaturization techniques for MIMO antenna systems have been investigated for ISM band operation, including 2.45- and/or 5-GHz ISM bands [18–21].

In [18], a 2×2 (four-element) MIMO patch antenna operating at 2.45-GHz ISM band and uses complementary split-ring resonator loaded on its ground plane for antenna miniaturization. As a result, the single-element antenna size is reduced by 76% with $100 \times 50 \times 0.8\,\text{mm}^3$ of a total size of the proposed MIMO antenna system. A minimum measured isolation of 10 dB is obtained given the close interelement spacing of 0.17λ. In another design [19], a dual-layer mushroom EBG structure was proposed and used to develop various 2-element and 4-element miniaturized microstrip patch antennas (MPAs) at 2.5 GHz with inter-element separation of 0.5λ. The mushroom inner layer provided the necessary antenna miniaturization and the upper layer helped in further mutual coupling reduction between the antenna elements. The designed multi-antennas, exhibiting low mutual coupling levels in the range of 28 dB to 50 dB, were 61% smaller in area than conventional MPAs and exhibited extremely low pattern correlations of 0.001.

Ref. [20] used a defected shorting wall between two elements of aperture-coupled patch antenna, separated by only 4 mm, to reduce an isolation by 20 dB, and for miniaturizing the system, two H-shaped slot feedings were employed. The envelope correlation coefficient (ECC) less than 0.01 is obtained. A two-element MIMO metamaterial-based antenna was presented by Abdalla and Ibrahim [21] for 5.8 GHz WiMAX applications. A one left-handed metamaterial unit cell and a simple defected ground structure between the two antenna elements, separated by only 1.8 mm are employed. A minimum isolation better than 45 dB and antenna size reduction more than 50% were attained compared to conventional patch antennas counterpart operating at the same frequency. From the literature survey, it is found that all these techniques have the problems of 1) requiring additional structures to reduce mutual coupling or antenna miniaturization, 2) being complex to be manufactured, or 3) being large in size.

Based on orthogonal polarization diversity, this paper presents a design of two- and four-element MIMO antennas operating at 5 GHz and covering (4–6) GHz band, with compact sizes, good isolations, and simple fabrication. In this work, the hexagonal geometry is adopted as a radiating element to design the MIMO antenna systems since it has smaller size and can be designed by using variation of

static energy below the square or circular monopole antennas [22]. In the MIMO system, each element is a hexagonal-ring monopole antenna (HRMA), and a CPW-fed line is used to feed this antenna. The HRMA has a size of only $13 \times 10\,\text{mm}^2$; meanwhile, a MIMO system is constituted from more than one of these symmetrical antenna elements, arranged in mutual orthogonal configuration, and the spacing between them is only 3 mm or $0.02\lambda_0$ at 5 GHz.

The primary aim of this paper is to introduce a new design approach for designing compact HRMA element. The design initially begins with a conventional reference antenna, stripline-fed circular monopole antenna (CMA), then the desired CPW-fed HRMA is designed with miniaturized size of 50% compared with the stripline-fed CMA counterpart. Two full-wave commercially software packages are used in this wok. The first one is a Computer Simulation Microwave Studio (CST MWS), and the second one, to validate the simulated results, is a High Frequency Structure Simulator (HFSS). For verification of simulation results, the single antenna element, HRMA, besides the two designs, 2×1 and 2×2 MIMO antenna systems, is fabricated, and the prototypes are measured. A good agreement is shown between simulated and measured results.

2. DESIGN OF A BASIC ANTENNA ELEMENT

The basic antenna element employed in the proposed MIMO system is based on coplanar waveguide (CPW)-fed hexagonal ring monopole antenna (HRMA). This section introduces the main concepts to design this basic antenna element starting from a stripline (SL)-fed circular monopole antenna (CMA). This represents the reference antenna (RA) for the next development. Then various antennas involved in the design evolution process are introduced aiming to achieve compact HRMA (50% reduction in area compared with RA). It is assumed that the specified information includes the dielectric constant of substrate ε_r, resonant frequency f_r, and the height of substrate h is given. The outline design procedure is as follows

(i) For designing HRMA element, first, two of CMAs are presented. One is based on SL-fed and called SL_CMA, and the other is based on CPW-fed and called CPW_CMA. They closely related to each other, and the size and parameter dimension values of them are equal. Initially, SL_CMA is designed to be resonated at the fundamental resonance frequency which is approximately given by [22]

$$f_r = \frac{X_{mn}}{2\pi a_e \sqrt{\varepsilon_r}} c \tag{1}$$

where f_r is the resonance frequency of the patch, $X_{mn} = 1.8411$ for the dominant mode TM_{11}, c the velocity of light in free space, ε_r the relative permittivity of the substrate and a_e the effective radius of the circular patch and given by

$$a_e = a \left\{ 1 - \frac{2h}{\pi a \varepsilon_r} \left(\ln \frac{\pi a}{2h} + 1.7726 \right) \right\}^{1/2} \tag{2}$$

In the above expression, 'a' is the actual radius of the circular patch antenna as shown in Fig. 1, whereas h is the height of the substrate. Eq. (1) can be applied to designing SL_CMA by relating the areas of the circular and hexagonal patches as shown in (3).

$$\pi a_e^2 = \frac{3\sqrt{3}}{2} s^2 \tag{3}$$

where s is the side length of the hexagonal patch.
In this paper, the reference antenna, SL_CMA (see Fig. 1) is designed to resonate at 5.0 GHz using a substrate having $h = 1.5$ mm and $\varepsilon_r = 4.3$ (FR4). Applying Eqs. (1) and (2) gives $a_e = 7.6$ mm and $f_r = 5.6$ GHz, whereas CST S_{11} simulation result in Fig. 2 shows that the antenna resonates at the lower TM_{11} mode resonance frequency $f_r = 5.0$ GHz. Thus, good agreement is achieved between simulated and theoretical results for designing the reference antenna.

(ii) The second step in the design procedure is to replace SL-fed by CPW-fed to produce CPW_CMA (see Fig. 1). It is seen from Fig. 2 that the CPW_CMA resonates at $f_r = 2.9$ GHz which is lower than the SL_CMA resonance frequency by a reduction in frequency more than 2 GHz.

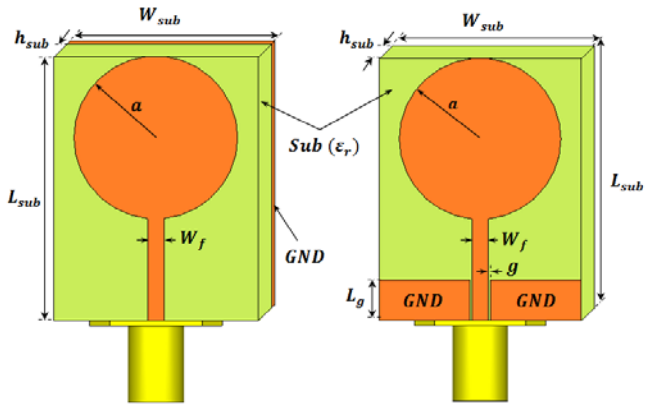

Figure 1. Proposed circular antenna element. (a) SL_CMA. (b) CPW_CMA. ($L_{sub} = 26\,\text{mm}$, $W_{sub} = 20\,\text{mm}$, $h_{sub} = 1.5\,\text{mm}$, $W_f = 2\,\text{mm}$, $a = 8\,\text{mm}$, $L_g = 4\,\text{mm}$, $g = 0.2\,\text{mm}$, $\varepsilon_r = 4.3$).

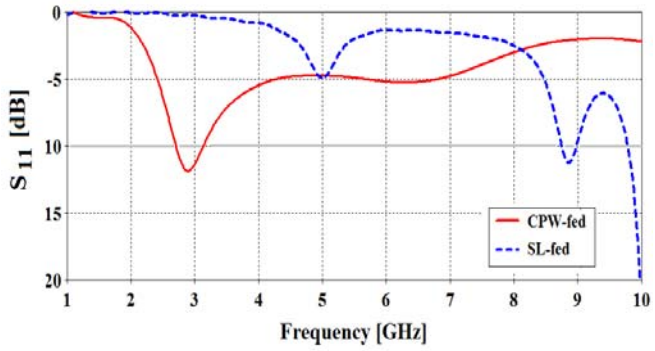

Figure 2. CST simulated S_{11} curves of circular patch antennas.

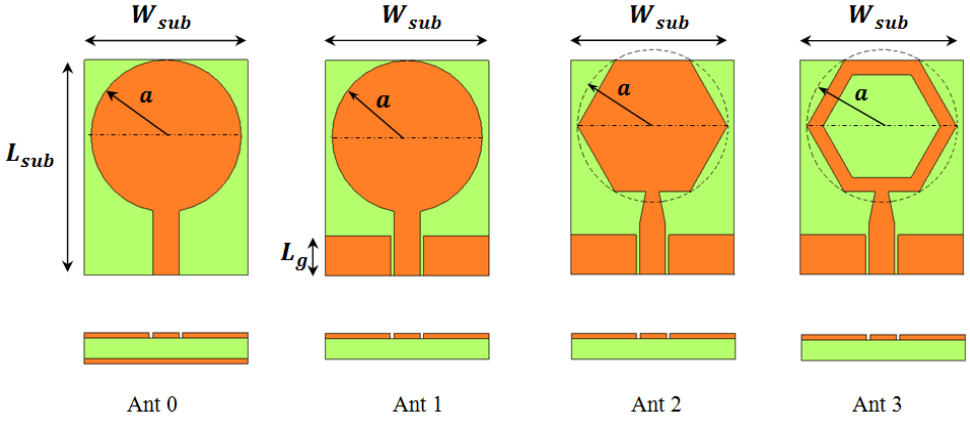

Figure 3. Geometry of various antennas involved in the design evolution. ($L_{sub} = 13\,\text{mm}$, $W_{sub} = 10\,\text{mm}$, $h_{sub} = 1.5\,\text{mm}$, $W_f = 2\,\text{mm}$, $a = 4.6\,\text{mm}$, $L_g = 2.4\,\text{mm} g = 0.2\,\text{mm}$, $\varepsilon_r = 4.3$).

(iii) In the third step, Ant 0 (SL_CMA) and Ant 1 (CPW_CMA), see Fig. 3, are redesigned by lowering their sizes from $26 \times 20\,\text{mm}^2$ to $13 \times 10\,\text{mm}^2$, i.e., 50% area reduction for each one compared with the RA counterpart at 5 GHz band. Fig. 4 shows that Ant 0 and Ant 1 have resonance TM_{11} modes of 8.75 GHz and 5.75 GHz, respectively.

(iv) The fourth step of the design is to replace the circular radiating structure by its equivalent area of hexagonal counterpart. Ant 2 is produced, and its lower resonance frequency occurs at 5.25 GHz as noticed in Fig. 4.

(v) In the fifth and final step of the proposed design procedure, Ant 3 (HRMA) is presented, and its resonance frequency is produced at 5 GHz, as shown in Fig. 4, which is our design goal, $f_r = 5$ GHz.

In this paper, the HRMA is adopted as a basic antenna element in the MIMO system since our intention is to reduce the total surface area of the metallic parts of the antenna. This is done by removing the metallization from the antenna's center since most of the surface current was concentrated along the edges of the hexagon structure, see Fig. 5(a). As a result, Ant 2 and Ant 3 are similar in their performance in terms of S_{11} and radiation patterns as noticed in Figs. 4 and 5(b), respectively. Hence reducing the metal content of the antenna speeds up the prototyping and fabrication process while using less metallization.

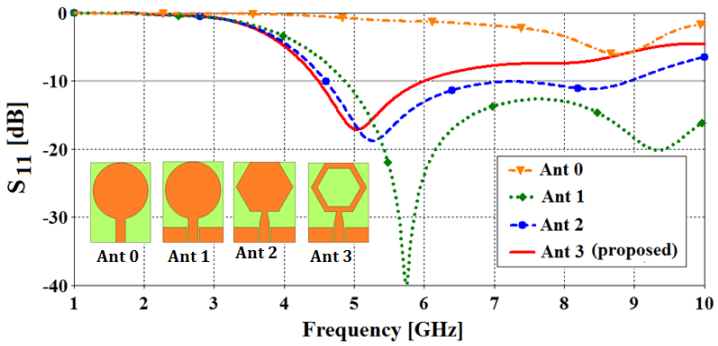

Figure 4. CST simulated return loss curves of various antennas.

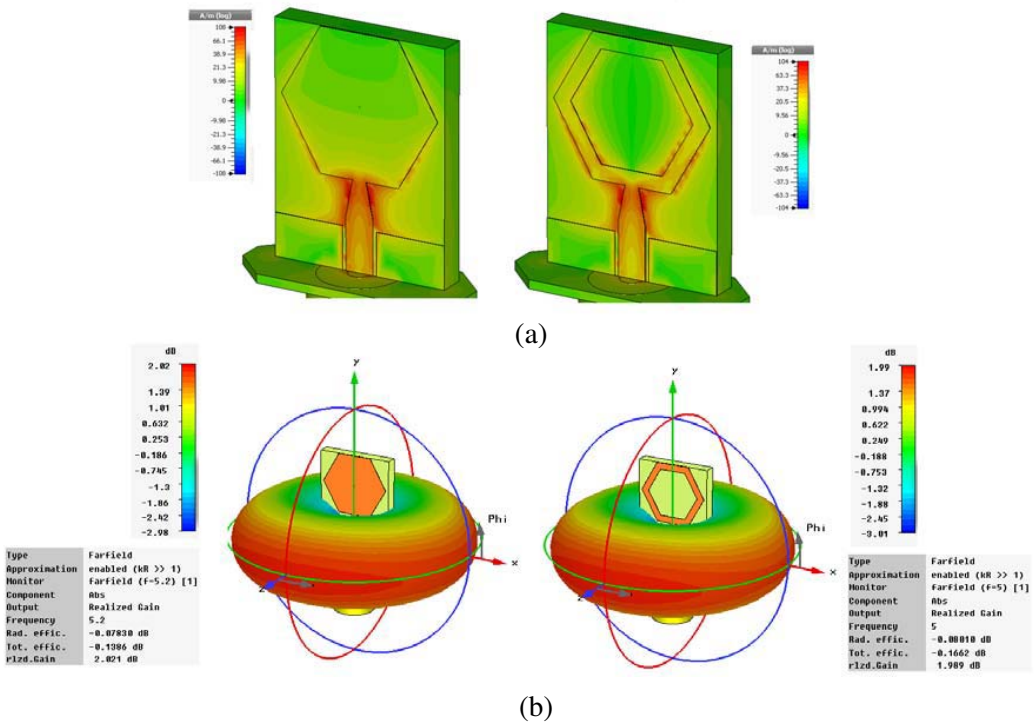

Figure 5. CST simulation of left Ant 2 (HMA), and right Ant 3 (HRMA). (a) Surface current distributions. (b) 3D radiation patterns.

3. STRUCTURE OF THE MIMO ANTENNAS

3.1. One-Element Antenna

Figure 6 shows the configuration of HRMA with detailed dimensions and parameters. A hexagonal ring-shaped structure fed by a coplanar waveguide (CPW) is adopted here as the radiating element since the CPW feeding mechanism usually outperforms microstrip-fed counterparts in terms of impedance matching, omnidirectional patterns and wider bandwidth. This simple design is shown in Fig. 6, whose conductor is fabricated on an inexpensive FR4 substrate with the dielectric constant of $\varepsilon_r = 4.4$ and substrate thickness of $h = 1.5\,\text{mm}$. The dimensions of the designed HRMA, including the substrate, are $L_{sub} \times W_{sub} = 13\,\text{mm} \times 10\,\text{mm}$ or about $0.21\lambda \times 0.16\lambda$ at 5 GHz. It is composed of a hexagonal ring radiating element, with a side length of $S = 4.6\,\text{mm}$ and a width of $t = 0.75\,\text{mm}$, a 50-Ω CPW-fed structure, and a symmetrical ground plane ($L_g = 2.5\,\text{mm}$). The 50-Ω CPW-fed structure, with width $W_1 = 2\,\text{mm}$ and length ($L_g + L_1 = 6\,\text{mm}$), is used to feed the antenna centrally from the bottom edge of the rectangular strip. A $g = 0.2\,\text{mm}$ gap is used between the signal strip and the coplanar ground plane. To provide a broadband behavior with a relatively good matching, the radiating element is connected to CPW-fed structure via a tapered line, narrow upper edge of width $W_2 = 1\,\text{mm}$.

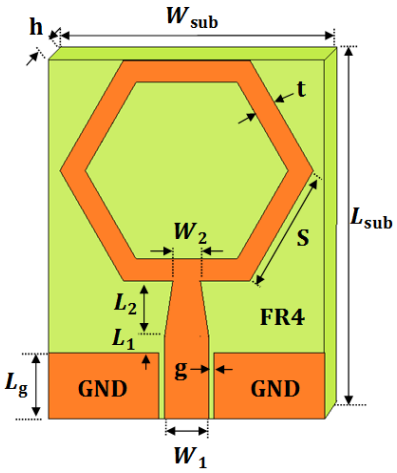

Figure 6. Schematic of the HRMA with its dimensions and parameters.

3.2. Two- and Four-Element MIMO Antenna Systems

The configuration and photograph of the fabricated of two- and four-element MIMO antenna systems along with single-element HRMA are shown in Figs. 7(a) and (b), respectively. In order to have orthogonal polarization, each antenna in the system has been arranged at a 90-degree angle to each other. The area of each antenna element is $13 \times 10\,\text{mm}^2$, and areas of the proposed MIMO systems are $13 \times 26\,\text{mm}^2$ (2-element) and $26 \times 26\,\text{mm}^2$ (4-element). The edge to edge separation between the antennas in the MIMO system is taken as $W_s = 3\,\text{mm}$ ($0.02\lambda_0$) at $f_0 = 5\,\text{GHz}$. The antennas are printed on one side of the substrate and fed with CPW structure. The SMA connector was included in the simulated model to improve the simulation precision. The final parameters of the antennas are listed in Table 1.

4. EXPERIMENTAL AND SIMULATION RESULTS OF THE MIMO ANTENNAS

The antenna shapes and their dimensions were first designed based on the CST MWS simulator package and then confirmed by using HFSS. To validate the simulated results, prototypes based on the dimensions in Fig. 7 and Table 1 are fabricated and measured. The S-parameters are measured by an Anritsu 3650A-1 vector network analyzer.

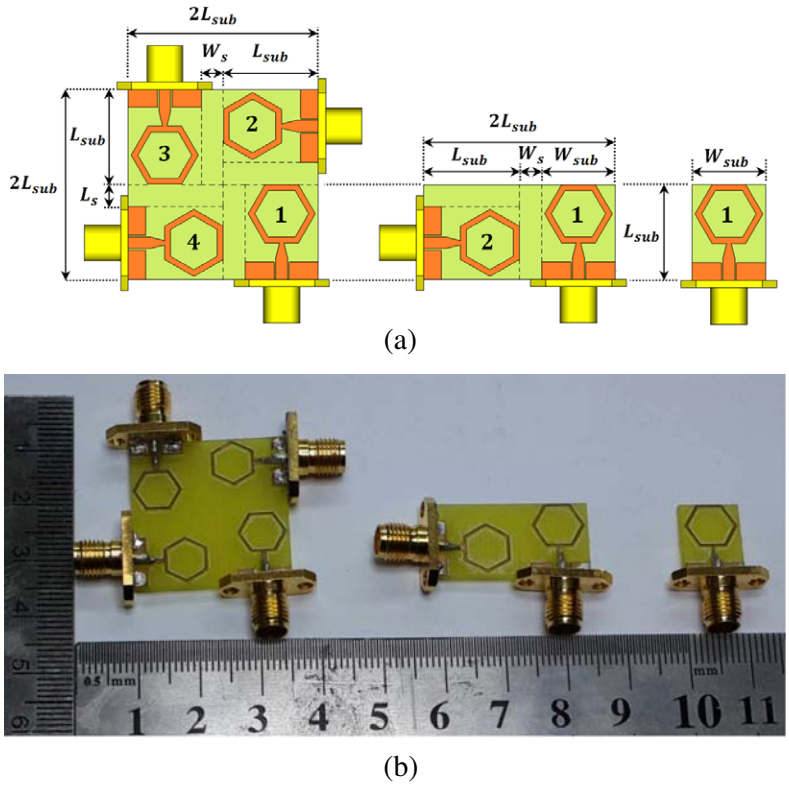

Figure 7. (a)Configuration of the proposed 2×1 and 2×2 MIMO antenna systems along with single-element antenna, with their dimensions and parameters. (b) Photograph of the fabricated MIMO antennas.

Table 1. Geometric parameters of the proposed MIMO antenna systems.

Parameters	Values (mm)	Parameters	Values (mm)
L_{sub}	13.0	W_1	1.6
W_{sub}	10.0	W_2	1.0
h_{sub}	1.5	W_s	3.0
L_g	2.4	L_s	3.0
L_1	0.6	t	0.75
L_2	2.0	g	0.2
S	4.6		

4.1. A Single-Element Antenna

The measured and simulated S_{11} curves by CST and HFSS for the single-element antenna are shown in Fig. 8. As can be noticed from this figure, the antenna resonates at 5 GHz, so the aim of design procedure has been satisfied. The CST (HFSS) -10-dB simulated impedance bandwidth covers frequency from 4.48 GHz (4.53 GHz) to 6.0 GHz (6.35 GHz), while the measured bandwidth covers from 4.53 to 5.76 GHz. It is seen that there is a good agreement between the two simulations with a small variation between them since different numerical techniques are used by the two softwares. The differences between the measured and simulated results, but follow the same pattern of simulated results, may come from the manufacture error and the uncertainty in relative dielectric constant ε_r and thickness of the substrate.

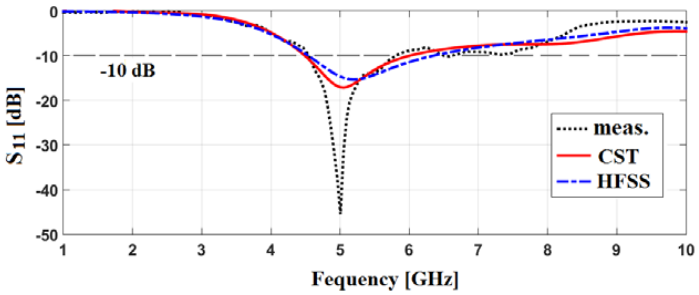

Figure 8. Measured and simulated S_{11} results of HRMA.

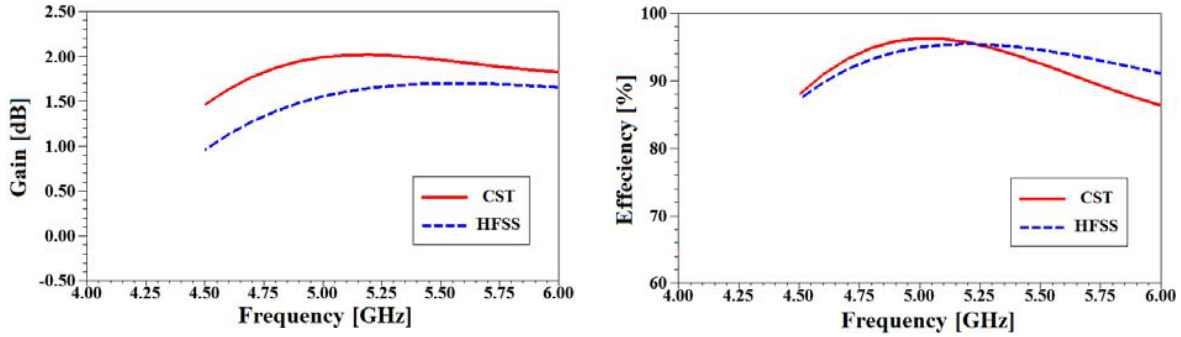

(a) (b)

Figure 9. CST and HFSS simulated results of (a) gain and (b) efficiency of the proposed HRPA.

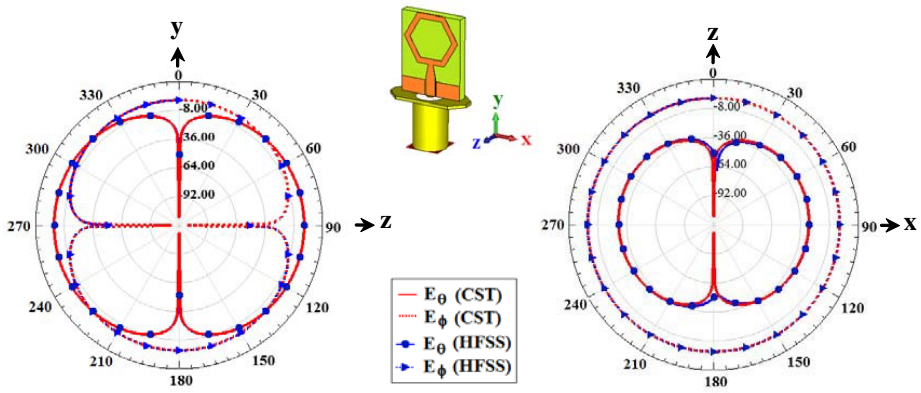

(a) (b)

Figure 10. CST and HFSS simulated directive gain pattern at 5 GHz of a single antenna element, HRMA. (a) E- or yz-plane. (b) H- or xz-plane.

Figure 9 shows the CST and HFSS simulated gain and efficiency of the proposed antenna at the 5-GHz ISM band. Part (a) of this figure shows that the gain is nearly constant for frequencies greater than 5 GHz, and the peak gain rises to 2.1 dBi (CST) and 1.6 dBi (HFSS). Fig. 9(b) shows that the efficiency remains above 85% in the working band and reaches around 95% at the peak. The simulated directive gain patterns of the single antenna in yz- and xy-planes at 5 GHz are shown in Fig. 10. The agreement between the results obtained from the CST and HFSS softwares is quite apparent. From observing parts (a) and (b) of this figure, the E-plane (yz) and H-plane (xy), respectively, the antenna has an omnidirectional radiation pattern over the entire operating frequency band.

4.2. A Two-Element Antenna

In this subsection, the performance results of a 2×1 MIMO antenna by using 2-element HRMA is presented and discussed. The measured and simulated S-parameter results of these two antennas are shown in Fig. 11(a). Based on measurement results, antenna 1 (antenna 2) operates in frequencies from 3.9 (4.3) to 6.4 GHz (6.6 GHz) with a resonance frequency of 4.4 GHz (4.8 GHz). The achieved bandwidths can cover 5-GHz (5.15–5.85 GHz) band for WLAN and WiMAX applications. Fig. 11(b) shows the isolation characteristics of each antenna element. The measured isolation is relatively weak with a maximum value of -15 dB over the entire range of frequencies (1 to 10 GHz). The low isolation between the elements in the system is due to the compact size of the antenna elements, which allows them to be closed to each other. Moreover, the CPW-fed technique is inherent in low isolation between closed elements.

The simulated gain and radiation efficiency for both antennas are plotted in Figs. 12(a) and (b), respectively. From Fig. 12(a), it can be observed that for excitation at port-2 (port-1), the gain is greater than 1.5 dBi (-0.5 dBi), and the maximum reaches 2.5 dBi (1.0 dBi) throughout the operating band (4–6 GHz). Fig. 12(b) shows that for excitation at port-2 (port-1), the efficiency stays above 80% (65%) in the band and reaches around 95% (90%) at the peak. The CST and HFSS far-field simulated directive gain patterns of the two-element MIMO antenna in both yz- and xz-planes at 5 GHz are shown in Figs. 13(a) and (b), for excitations at port-1 and port-2, respectively. It is seen that similar results are obtained from the CST and HFSS softwares. As shown from the two figures, a small variation with respect to those obtained from single-element is shown in Fig. 10. Also, an orthogonality in radiation patterns of the two antenna elements is observed in both planes, yz (elevation) and xz (azimuth).

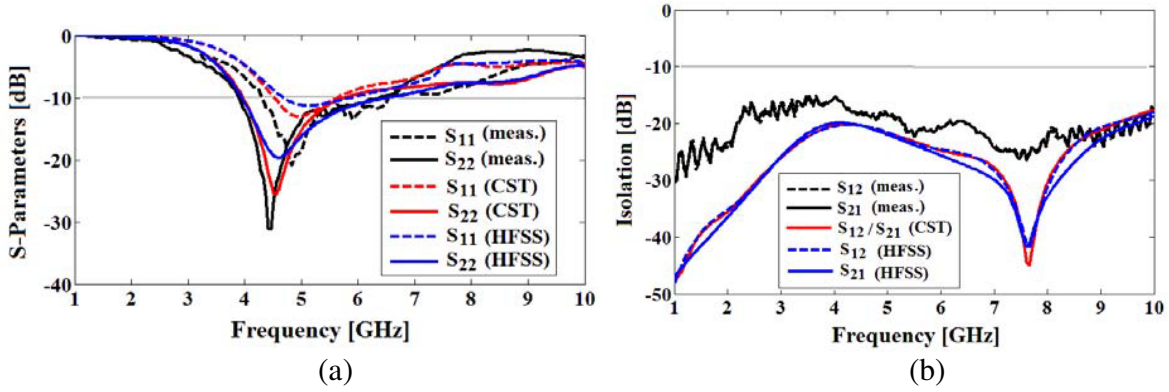

Figure 11. Measured and simulated results of the proposed 2×1 MIMO antenna system. (a) S-parameters. (b) Isolation.

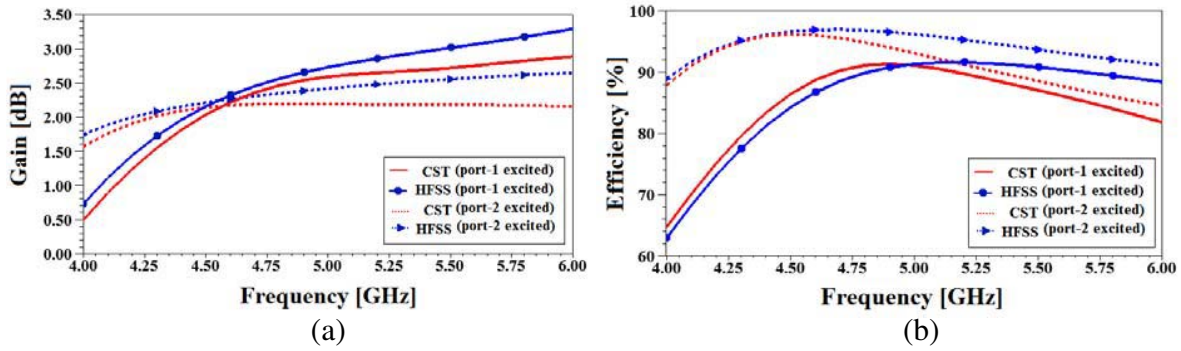

Figure 12. CST and HFSS simulated results of (a) gain and (b) efficiency of the 2-element MIMO system.

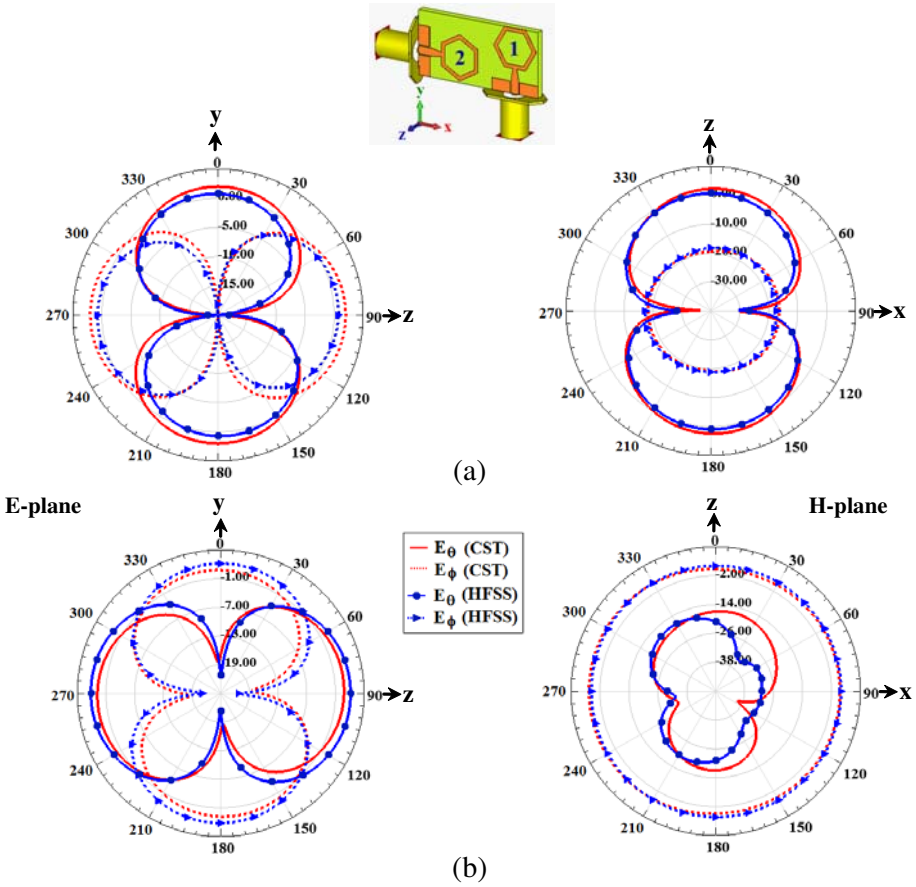

Figure 13. CST and HFSS simulated directive gain patterns at 5 GHz of a 2-element MIMO system. (a) Port-1 excited and (b) port-2 excited.

4.3. A Four-Element Antenna

Using a HRMA, the element proposed in Section 2, a four-element MIMO antenna is built, and its structure is shown in Fig. 7. As stated before, this antenna is fabricated on a 1.5-mm thick FR-4 substrate, and the four elements are rotationally symmetrically placed with an interval of 90°. Figs. 14(a) and (b) show the measured and simulated results of the S-parameters and isolation curves of the 2×2 MIMO antenna system, respectively. It is shown from Fig. 14(a) that the four antennas are resonating at TM_{11} frequency mode of ~ 4.5 GHz, and their -10 dB impedance bandwidth is ~ 2 GHz ranging from 4 to 6 GHz. It can be observed from Fig. 14(b) that an isolation better than 15 dB is attained throughout the full frequency range (1 to 10 GHz) for antenna spacing of $0.02\lambda_0$, where λ_0 is the centered wavelength of the designed antenna. Although CST and HFSS simulation models of a MIMO antenna system are carried out with the SMA connector, some variations in simulated and measured S-parameters and isolation curves are observed. This is due to fabrication tolerances associated with the compactness of the design that provided rounded corners while simulation expected sharp edges. Anyway, a reasonable agreement between the measurement and simulation results is obtained, validating the HFSS and CST models. In the simulation and measurement, S_{ii} curves, $i = 1, 2, 3$ or 4 are obtained when the standard 50-Ω matching load is used to terminate three ports whereas the other port is excited. And, S_{ij} (isolation) curves, $j = 1, 2, 3$ or 4 and $i \neq j$, are obtained with a two-port VNA by switching between the antenna ports, 2 by 2, whereas the other two ports are kept with a SMA 50-Ω load. Due to the symmetry of the antenna elements, some of the isolation curves are similar to each other. Thus, only four curves, S_{12}, S_{13}, S_{23}, and S_{24}, are needed to be plotted for simulation and measurement, as depicted in Fig. 14(b).

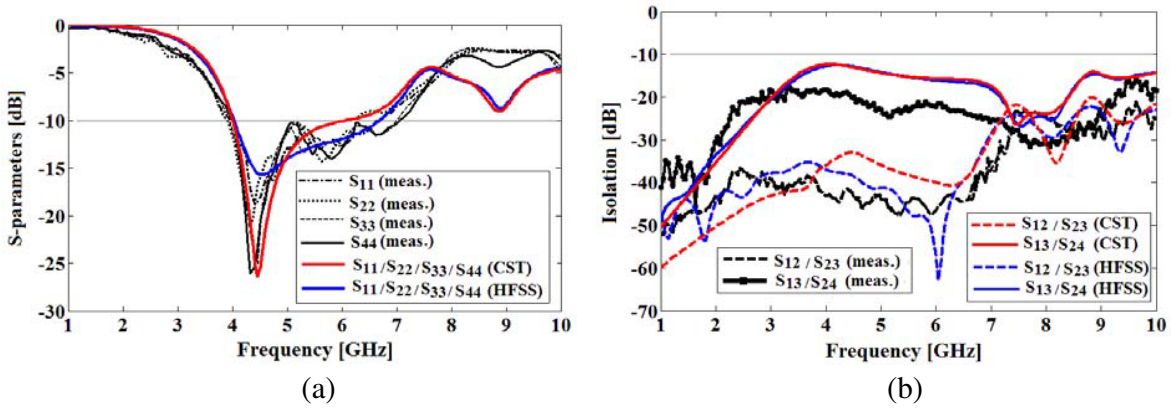

Figure 14. Measured and simulated results of the proposed 2×2 MIMO antenna system. (a) S-parameters. (b) Isolation.

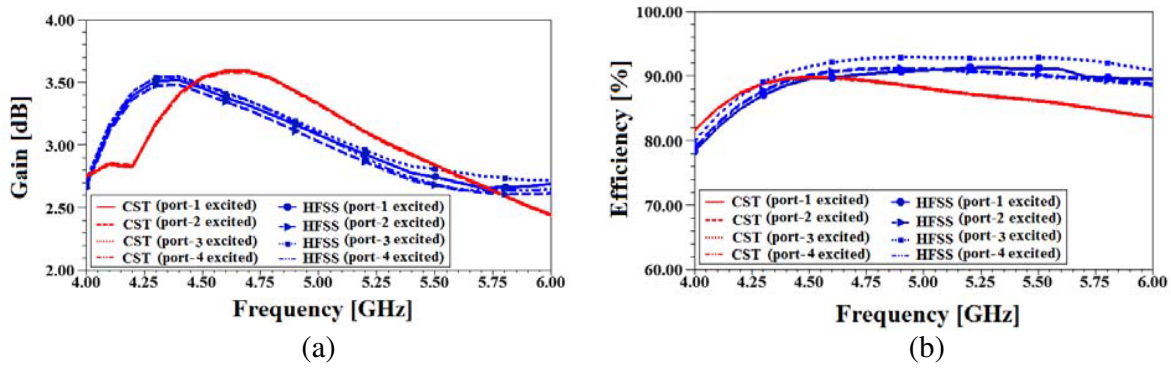

Figure 15. CST and HFSS simulated results of (a) gain and (b) efficiency of the 4-element MIMO system.

The simulated realized peak gains and efficiencies of the four-element MIMO antenna, with antenna under test excited and the remaining antennas terminated by a matched load, are shown in Figs. 15(a) and (b), respectively. It can be observed from Fig. 15(a) that the CST and HFSS simulated peak gain curves agree well, but their maximum values of 3.6 dBi occur at 4.3 and 4.7 GHz, respectively. Fig. 15(a) also shows that the peak gain curves of the antennas are quite similar and remain above 2.5 dBi across the frequency band from 4–6 GHz. It can be seen from Fig. 15(b) that simulated efficiencies (in both CST and HFSS packages) are above 80% across the operating band. The CST and HFSS simulated antenna's efficiency curves nearly coincide with each other at lower frequencies in the operating band (4–4.3 GHz), and they differ slightly from each other at higher frequencies in the band (4.3–6 GHz).

Simulated (CST and HFSS) radiation patterns for two principal planes, E- and H-plane, for each antenna element when one antenna is excited and the other three antennas terminated by a matching load, are shown in Fig. 16. It is seen from the figure that nearly omnidirectional pattern is attained at 5 GHz, the centered frequency of the designed antennas. Also, Fig. 16 indicates that the antennas have orthogonal radiation patterns which reduce signal correlation between antenna elements and enhance the antennas' input impedance matching. Thus, the combination of closely spaced antennas in a compact configuration with orthogonal radiation patterns may lead to high antenna isolation characteristics [23].

5. DIVERSITY PERFORMANCE OF MIMO ANTENNAS AND SIZE COMPARISON

The antenna diversity represents an important parameter that describe the performance of the MIMO antenna system. There are three main ways to realize the antenna diversity that can be employed by

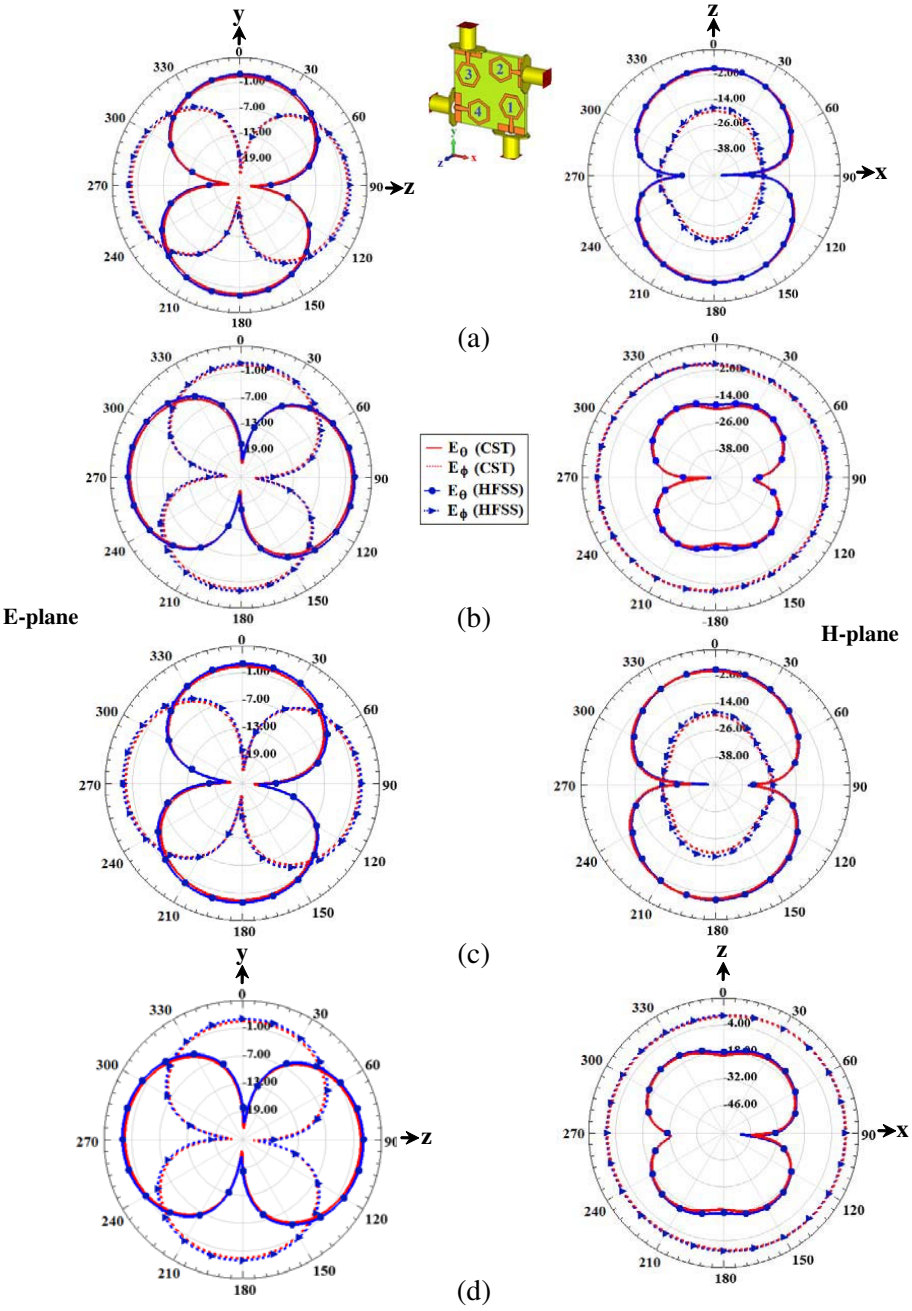

Figure 16. CST and HFSS simulated directive gain patterns at 5 GHz of a 4-element MIMO system. (a) Port-1 excited. (b) Port-2 excited. (c) Port-3 excited and (d) port-4 excited.

designers to improve signal quality and further increase system reliability [24].

(i) *Spatial diversity* uses multiple antennas having the same characteristics and physically separated by the order of a wavelength from one another. This type of diversity permits multiple users to share a limited communication spectrum and avoid co-channel interference.

(ii) *Pattern diversity* comprises two or more antennas having different directive radiation patterns and physically separated by some (often short) distance. Such diversity results in almost a large portion of angle space can provide a higher gain and 360-degree coverage in the azimuthal plane, compared to a single omnidirectional antenna.

(iii) *Polarization diversity* combines one or two pairs of identical antennas with orthogonal polarizations,

a polarization difference of 90°, (i.e., horizontal/vertical or Left-hand/Right-hand circular polarization). By employing pairs of complementary polarizations, this scheme prevents a system from polarization mismatches, and reduction in mutual coupling between adjacent antennas can be achieved.

Based on previous discussion, a polarization diversity technique is used in this paper to enhance the isolation performance between closely spaced antennas. Usually, envelope correlation coefficient (ECC) is the measure of isolation between any two antenna elements. It gives a measure of how much the antenna elements in MIMO system are coupled to each other. A lower ECC results in better use of antenna diversity. Generally, two methods were used in the literatures to compute ECC, from either 3D far-field radiation patterns [25] or S-parameters [26]. Practically, the measurements of the 3D far-field radiation pattern is more complicated than S-parameters as a result, and the S-parameters based ECC computation is preferred. Based on S-parameters in [26], the ECC (ρ_e) between antennas i and j in an N-element MIMO antenna system can be computed:

$$\rho_e(i,j,N) = \left| \frac{\sum_{n=1}^{N} S_{i,n}^* S_{n,j}}{\left| \prod_{k=i,j} \left(1 - \sum_{n=1}^{N} S_{k,n}^* S_{n,k}\right) \right|^{1/2}} \right|^2 \tag{4}$$

For a 2-element MIMO antenna system, $i, j = 1$ or 2 and $N = 2$, Eq. (4) becomes

$$\rho_e(1,2,2) = \frac{\left|S_{11}^* S_{12} + S_{21}^* S_{22}\right|^2}{\left(1 - |S_{11}|^2 - |S_{21}|^2\right)\left(1 - |S_{22}|^2 - |S_{12}|^2\right)} \tag{5}$$

As well, the ECC or ρ_e for a 4-element MIMO antenna system is computed from applying Eqs. (6) and (7), by substitution in Eq. (4), $N = 4$ and $i, j = 1, 2, 3$ or 4. In Eq. (5), $\rho_e(1,2,2)$ represents the envelope correlation between antennas 1 and 2 in a 2-element MIMO antenna system. On the other hand, in Eqs. (6) and (7), $\rho_e(1,2,4)$ and $\rho_e(1,3,4)$ are ECC-based computations for a 4-element MIMO antenna system between antennas 1, 2, and antennas 1, 3 (antenna number is illustrated in Fig. 8(a)), respectively.

$$\rho_e(1,2,4) = \frac{\left|S_{11}^* S_{12} + S_{21}^* S_{22} + S_{13}^* S_{32} + S_{14}^* S_{42}\right|^2}{\left(1 - |S_{11}|^2 - |S_{21}|^2 - |S_{31}|^2 - |S_{41}|^2\right)\left(1 - |S_{12}|^2 - |S_{22}|^2 - |S_{32}|^2 - |S_{42}|^2\right)} \tag{6}$$

$$\rho_e(1,3,4) = \frac{\left|S_{11}^* S_{13} + S_{21}^* S_{23} + S_{13}^* S_{33} + S_{14}^* S_{43}\right|^2}{\left(1 - |S_{11}|^2 - |S_{21}|^2 - |S_{31}|^2 - |S_{41}|^2\right)\left(1 - |S_{13}|^2 - |S_{23}|^2 - |S_{33}|^2 - |S_{43}|^2\right)} \tag{7}$$

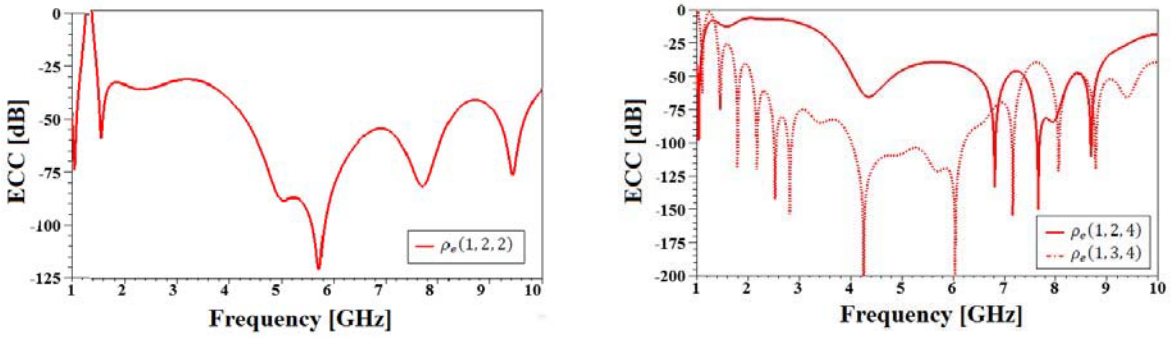

(a) (b)

Figure 17. The CST MWS simulated ECC for the proposed MIMO antenna system. (a) Two-element antenna. (b) Four-element antenna.

By applying Eqs. (5)–(7), the ECC based-CST MWS simulated S-parameters of 2- and 4-element MIMO antenna systems across the desired frequency band are plotted in Figs. 17(a) and (b), respectively. As can be observed, the value of ECC throughout the operating band is well below the practical threshold value of 0.5 ($\cong -6\,\text{dB}$), indicating that the proposed MIMO antenna systems have good diversity performance.

Table 2 presents a comparison between the proposed antenna and some other MIMO antennas reported in the literature in terms of size, bandwidth, and isolation. It is worth to emphasize here that the proposed printed MIMO antenna has the smallest area among previous antennas listed in Table 2. It is characterized by reasonable isolation and omnidirectional radiation patterns.

Table 2. Comparison between the proposed antenna and other printed MIMO antennas reported in literatures ($N > 2$).

Ref.	Aim	Antenna Structure	Center Frequency (in GHz)	Number of Element	Area (in λ^2)	Area Per Element (in λ^2)	Maximal Isolation (in dB)	(-10 dB Bandwidth) (in GHz)
This paper	Compact size	CPW-fed hexagonal-ring monopole antenna	5.000	4	0.187	0.035	−15.00	(4.000–6.000)
[6]	Compact size and improved isolation	Modified E-shaped patch antenna	6.950	2	2.466	0.740	−33.00	(6.100–7.800)
[13]	Compact size	E-shaped patch antenna	5.750	4	0.421	0.082	−22.00	(5.620–5.875)
[27]	Compact size and dual-band	CPW-fed Semicircle monopole antenna	2.530, 5.300	4	0.524	0.055	−23.25	(2.270–2.530) (5.030–5.530)
[28]	Compact size and directive gain	H-shaped directive antenna	5.550	4	0.593	0.116	−17.00	(5.100–6.000)
[29]	Compact size and dual-band	CPW-fed Slot antenna	2.525, 5.650	4	0.436	0.039	−29.00	(2.100–2.950) (5.050–6.250)

6. CONCLUSION

In this paper, a new design approach for compact MIMO antenna systems is presented. First, a stripline-fed patch antenna with circular shape was designed to resonate at 5 GHz. This represents the reference antenna for next development. At the end of the evolution design approach, a CPW-fed monopole antenna with hexagonal-ring (HRMA) is achieved. This HRMA represents a basic antenna element characterized by compact size (50% reduction in overall size in comparison with the reference antenna), simple structure, low profile, and low fabrication cost. Measurement results demonstrate that the basic antenna element has good omnidirectionality and satisfactory antenna return loss and bandwidth.

Based on diversity technique, two- and four-element MIMO systems, with closely spaced identical HRMAs and a polarization difference of 90° between them, are investigated and experimentally demonstrated for 5-GHz ISM band. The measured results of the two- and four-port MIMO antenna

systems agree well with the CST MWS and HFSS simulation results. Based on measurement results, the proposed MIMO antenna systems have good radiation characteristics and wide enough bandwidth of 2 GHz (4 to 6 GHz). Besides, these antennas show good isolation less than 15 dB and low envelope correlation coefficient better than −26 dB across the operating frequency band. Therefore, the proposed antenna can be used for the 5-GHz ISM band operations, which are required for the 5.2/5.8 GHz WLAN and 5.5 GHz WiMAX systems for MIMO applications in compact portable devices.

ACKNOWLEDGMENT

The author would like to thank Electronics Manufacturing Center, Industrial Development and Research of the Ministry of Science and Technology (MOST), Iraq for providing the fabrication and measurement facilities. The author acknowledges gratefully the help provided by Ghaleb N. Radad and Mahmood R. Muhsen from the MOST for their help in the fabrication and measurement of the prototype.

REFERENCES

1. Han, W., X. Zhou, J. Ouyang, Y. Li, R. Long, and F. Yang, "A six-port MIMO antenna system with high isolation for 5-GHz WLAN access points," *IEEE Antennas Wireless Propag. Lett.*, Vol. 13, 880–883, 2014.
2. Malik, J., A. Patnaik, and M. V. Kartikeyan, "Novel printed MIMO antenna with pattern and polarization diversity," *IEEE Antennas Wireless Propag. Lett.*, Vol. 14, 739–742, 2015.
3. Akdagli, A. and A. Toktas, "Design of wideband orthogonal MIMO antenna with improved correlation using a parasitic element for mobile handsets," *International Journal of Microwave and Wireless Technologies*, Vol. 7, 1–7, 2014.
4. Marzudi, W. N. N. W., Z. Z. Abidin, S. H. Dahlan, M. Yue, R. A. Abd-Alhameed, and M. B. Child, "A compact orthogonal wideband printed MIMO antenna for WiFi/WLAN/LTE applications," *Microwave Opt. Technol. Lett.*, Vol. 57, No. 7, 1733–1738, Jul. 2015.
5. See, C. H., R. A. Abd-Alhameed, N. J. McEwan, S. M. R. Jones, R. Asif, and P. S. Excell, "Design of a printed MIMO/diversity monopole antenna for future generation handheld devices," *International Journal of RF and Microwave Computer-Aided Engineering*, Vol. 24, No. 3, 348–359, May 2014.
6. Babu, K. J., R. W. Aldhaheri, M. Y. Talha, and I. S. Alruhaili, "Design of a compact two element MIMO antenna system with improved isolation," *Progress In Electromagnetics Research Letters*, Vol. 48, 27–32, 2014.
7. Li, Z., Z. Du, M. Takahashi, K. Saito, and K. Ito, "Reducing mutual coupling of MIMO antennas with parasitic elements for mobile terminals," *IEEE Trans. Antennas Propag.*, Vol. 60, No. 2, 473–481, Feb. 2012.
8. Li, J.-F., Q.-X. Chu, and T.-G. Huang, "A compact wideband MIMO antenna with two novel bent slits," *IEEE Trans. Antennas Propag.*, Vol. 60, No. 2, 482–489, Feb. 2012.
9. Su, S.-W., C.-T. Lee, and F.-S. Chang, "Printed MIMO-antenna system using neutralization-line technique for wireless USB-dongle applications," *IEEE Trans. Antennas Propag.*, Vol. 60, No. 2, 456–463, Feb. 2012.
10. Wang, Y. and Z. Du, "A wideband printed dual-antenna with three neutralization lines for mobile terminals," *IEEE Trans. Antennas Propag.*, Vol. 62, No. 3, 1495–1500, Mar. 2014.
11. Zhao, L. and K.-L. Wu, "A dual-band coupled resonator decoupling network for two coupled antenna," *IEEE Trans. Antennas Propag.*, Vol. 63, No. 7, 2843–2850, Jul. 2015.
12. Zhang, Z., H. Wang, and Z. Feng, "Dual-port planar MIMO antenna with ultra-high isolation and orthogonal radiation patterns," *Electronics Letters*, Vol. 51, No. 1, 7–8, Jan. 2015.
13. Mallahzadeh, A. R., S. Es'haghi, and A. Alipour, "Design of an E-shaped MIMO antenna using IWO algorithm for wireless application at 5.8 GHz," *Progress In Electromagnetics Research*, Vol. 90, 187–203, 2009.

14. Ryan, C. G. M. and G. V. Eleftheriades, "Two compact, wideband, and decoupled meander-lin antennas based on metamateria concepts," *IEEE Antennas Wireless Propag. Lett.*, Vol. 11, 1277–1280, 2012.
15. Zhang, X.-Y., X. Zhong, B. Li, and Y. Yu, "A dual-polarized MIMO antenna with EBG for 5.8 GHz WLAN application," *Progress In Electromagnetics Research Letters*, Vol. 51, 15–20, 2015.
16. Wang, K., R. A. M. Mauermayer, and T. F. Eibert, "Compact two-element printed monopole array with partially extended ground plane," *IEEE Antennas Wireless Propag. Lett.*, Vol. 13, 138–140, 2014.
17. Poole, I., "IEEE 802.11ac Gigabit Wi-Fi," 2013 [Online], Avaible: http://www.radio-electronics.com/info/wireless/wi-fi/ieee-802-11acgigabit.php.
18. Sharawi, M. S., M. U. Khan, A. B. Numan, and D. N. Aloi, "A CSRR loaded MIMO antenna system for ISM band operation," *IEEE Trans. Antennas Propag.*, Vol. 61, No. 8, 4265–4274, Aug. 2013.
19. Ghosh, S., T.-N. Tran, and T. L.-Ngoc "Dual-layer EBG-based miniaturized multi-element antenna for MIMO systems," *IEEE Trans. Antennas Propag.*, Vol. 62, No. 8, 3985–3997, Aug. 2014.
20. Dai, X.-W., L. Li, Z.-Y. Wang, and C-H. Liang, "High isolation and compact MIMO antenna system with defected shorting wall," *International Journal of Microwave and Wireless Technologies*, Vol. 7, 1–6, 2014.
21. Abdalla, M. A. and A. A. Ibrahim, "Compact and closely spaced metamaterial MIMO antenna with high isolation for wireless applications," *IEEE Antennas Wireless Propag. Lett.*, Vol. 12, 1452–1455, 2013.
22. Kushwaha, N. and R. Kumar, "Design of slotted ground hexagonal microstrip patch antenna and gain improvement with FSS screen," *Progress In Electromagnetics Research B*, Vol. 51, 177–199, 2013.
23. Karimian, R., H. Oraizi, S. Fakhte, and M. Farahani, "Novel F-shaped quad-band printed slot antenna for WLAN and WiMAX MIMO systems," *IEEE Antennas Wireless Propag. Lett.*, Vol. 12, 405–408, 2013.
24. Moon, J. and Y. Kim, "Antenna diversity strengthens wireless LANs," *Communication Systems Design*, 15–22, Jan. 2003.
25. Kulkarni, A. and S. K. Sharma, "A multiband antenna with MIMO implementation for USB dongle size wireless devices," *Microw. Opt. Technol. Lett.*, Vol. 54, No. 8, 1990–1994, Aug. 2012.
26. Blanch, S., J. Romeu, and I. Corbella, "Exact representation of antenna system diversity performance from input parameter description," *Electronics Letters*, Vol. 39, No. 9, 705–707, May 2003.
27. Fakhr, R. S., A. A. Lotfi-Neyestanak, and M. Naser-Moghadasi, "Compact size and dual band semicircle shaped antenna for MIMO applications," *Progress In Electromagnetics Research C*, Vol. 11, 147–154, 2009.
28. Luo, Y., Q.-X. Chu, J.-F. Li, and Y.-T. Wu, "A planar H-shaped directive antenna and its application in compact MIMO antenna," *IEEE Trans. Antennas Propag.*, Vol. 63, No. 9, 4810–4814, 2013.
29. Moghadasi, M. N., A. Danideh, A. Bakhtiari, and R. Sadeghifakhr, "Compact slot antenna for MIMO applications in the WLAN bands," *Microwave Opt. Technol. Lett.*, Vol. 55, No. 10, 2490–2493, Oct. 2013.